Genetic polymorphisms in SLCO2B1 and ABCC1 conjointly modulate atorvastatin intracellular accumulation in HEK293 recombinant cell lines

Laure Elens (laure.elens@uclouvain.be)
Université catholique de Louvain (UCLouvain)
Emilia Hoste
Université catholique de Louvain (UCLouvain)
Adrien Paquot
Université catholique de Louvain (UCLouvain)
Nadtha Panin
Université catholique de Louvain (UCLouvain)
Shaleena Horion
Université catholique de Louvain (UCLouvain)
Halima El Hamdaoui
Université catholique de Louvain (UCLouvain)
Giulio G Muccioli
Université catholique de Louvain (UCLouvain)
Vincent Haufroid
Université catholique de Louvain (UCLouvain)

Article

Keywords:

Posted Date: April 27th, 2022

DOI: https://doi.org/10.21203/rs.3.rs-1520877/v1

Version of Record: A version of this preprint was published at Therapeutic Drug Monitoring on October 11th, 2022. See the published version at https://doi.org/10.1097/FTD.0000000000001043.

Abstract

Atorvastatin (ATV), is commonly used to treat hypercholesterolemia. Although generally well tolerated, patients can suffer from muscle complaints and the occurrence of this discomfort is difficult to predict. Muscle side effects are assumed to be linked to the intramuscular ATV accumulation. The aim of our study was to investigate the relative implication of influx and efflux transporters expressed in the muscle tissue (OATP2B1, MRP1) in promoting or limiting the access of the drug into the cells. In addition, the impact of common single nucleotide polymorphisms (SNPs) in *SLCO2B1* coding for OATP2B1 (rs12422149; c.935G > A) and in *ABCC1* coding for MRP1 (rs45511401; c.2012G > T) was evaluated. Single or double transfectant HEK293 recombinant models overexpressing variant or wild-type OATP2B1 (influx) and/or MRP1 (efflux) proteins were developed. Our results confirm the implication of both OATP2B1 and MRP1 in ATV transport. Interestingly, ATV intracellular accumulation promoted by OATP2B1 influx was counteracted by MRP1 efflux. The c.935G > A SNP in *SLCO2B1* was associated with a decreased OATP2B1 influx activity whereas the c.2012G > T SNP in *ABCC1* appeared to increase MRP1 efflux activity towards ATV. In conclusion, intracellular ATV accumulation is regulated by transporter proteins and their functionality could play a role in ATV muscle side effect susceptibility.

Introduction

Atorvastatin (ATV), an HMG-CoA reductase inhibitor, commercialized under the name of statins, has proved its efficacy to reduce increased blood levels of low-density lipoprotein (LDL)-cholesterol and to limit the risk of cardiovascular diseases (CVD) [1, 2]. Although generally well tolerated, 10 to 25% of the patients might suffer from muscle complaints and/or myotoxicities, a relatively uncomfortable side-effect that can eventually lead to spontaneous patient poor compliance [3, 4]. As an HMG-CoA reductase inhibitor, ATV competitively inhibits the mevalonate pathway implicated in the cholesterol synthesis [5]. While ATV mediated-HMG-CoA reductase inhibition is related to its effect on cholesterol synthesis, it is thought to also account for its adverse effects, among which muscular complains. Indeed, the ATV-mediated inhibition of the mevalonate pathway, and the consequent downstream metabolite depletion, leads to a joint reduction of their respective physiological activity that might constitute a possible explanation for ATV-related muscular side effects [6]. ATV-mediated HMG-CoA reductase inhibition and the resulting metabolite depletion is known to be dose-dependent [1]. This suggests that understanding the ATV intracellular pharmacokinetics (PK), and the factors affecting it, is essential to unravel the reasons of treatment response variabilities and the susceptibility to muscle side effects. More particularly, the fact that statin-induced myopathy (SIM) is specific to the skeletal muscle tissue, and is dose- and drug potency-dependent [7–9], provides rationale to explore the importance of factors affecting intra-myocyte concentrations. ATV can enter in the myocytes, where toxicity occurs, by passive diffusion. However, some data also suggest that active transport can be a preponderant mechanism [10]. The activity of transporters expressed in skeletal muscle tissue is thus assumed to modulate drug concentrations directly within myocytes through both drug efflux and influx. Among efflux transporters implicated in ATV PK, MRP1, encoded by *ABCC1* (ATP-binding cassette sub-family C, member 1), is one of

the most expressed whereas OATP2B1, encoded by *SLCO2B1* (solute carrier organic anion sub-family 2B, member 1) is, to our knowledge, the only drug influx transporter involved in ATV transport and expressed in skeletal muscle tissues [11]. This suggests a role for these transporters in protecting or sensitizing myocytes from statin toxicity but the correlation between transporter activity and ATV cellular disposition has poorly been explored. Also, an unexplored question is the potential impact of functional single nucleotide polymorphisms (SNPs) on the role of these transporters in driving the drug across membranes and determining drug cellular accumulation and possibly explaining inter-individual differences regards to the risks of muscle side effects. *ABCC1* is located on the chromosome 16p13.11, and contains 34 exons (NG_028268.2). This efflux transporter transport various molecules such as ions, glutathione or xenobiotics [12]. ABCB1 expression is relatively ubiquitous however its expression is more important in the lungs, on the basolateral membranes of proximal renal tubular cells and of epithelial cells of the small intestine but is not found in the liver [13]. *ABCC1* is highly polymorphic. Among others, the rs45511401 (c.2012G > T, Gly671Val) SNP is a non-synonymous coding SNP located close to the first nucleotide-binding domain of the protein [14]. OATP2B1 is an influx drug carrier that transports endogenous (e.g. estrone-3-sulfate, pregnenolone sulfate) as well as exogenous (e.g. ATV, rosuvastatin) substrates. Its coding gene (*SLCO2B1*) is located on the chromosome 11q13.4, that counts 16 exons (NG_027921.1) [15]. This influx transporter is mainly expressed on the basolateral hepatic membranes facilitating the extraction of endogenous substrates and drugs from the blood to the hepatocyte for further metabolization [16, 17]. It is also expressed in the skeletal muscle tissue, in the blood-brain barrier, the kidney, the small intestine and, to a lesser extent, in the placenta [18]. Since the protein is not very well characterized, few data are available. However, the non-synonymous SNP rs12422149 (c.935G > A, Arg312Gln) in *SLCO2B1* has been described to be associated with increased simvastatin plasma levels and with reduced rosuvastatin efficiency, suggesting a significant impact of this SNP on the PK of its substrates [19, 20]. However, to date, no data on ATV are available.

Both polymorphisms are commonly found in the general population (Table 1). The minor allele frequency for rs45511401 in *ABCC1* is higher in European population (4.6%) than that of American (2%), South Asian (1.1%) or African (0.5%) with a global minor allelic frequency of about 2%. Minor allele frequency for rs12422149 in *SLCO2B1* is globally higher (21%). With a very high frequency in American (36.5%) and in South-East Asian populations (26.3% and 32% respectively) and a lower frequency in African and European (9.2 and 9.5%) [21, 22].

Table 1
Minor allele frequency (MAF) among ethnicities for rs45511401 in *ABCC1* and rs12422149 in *SLCO2B1* according to Ensembl.org.

rs45511401 in *ABCC1*		**rs12422149 in *SLCO2B1***	
Global	**0.015**	**Global**	**0.210**
European	0.046	European	0.095
American	0.020	American	0.365
African	0.005	African	0.092
South Asian	0.011	South Asian	0.263
East Asian	0	East Asian	0.320

The goal of the present study is to assess the activity of both transporters and the functional effect of 2 common non-synonymous coding SNPs on ATV cellular transport. In that context, *in vitro* recombinant models overexpressing the transporters either separately (single transfectants) or simultaneously (double transfectants), were developed by stable transfection in HEK293 cells.

Results

Generation of stable $SLCO2B1_{935G}$ and $SLCO2B1_{935A}$ overexpressing cell lines and characterization of OATP2B1 expression level

After transfection of HEK293 with pCMV-V-OFPSpark® containing the coding sequence $SLCO2B1_{935G}$ or $SLCO2B1_{935A}$, similar OATP2B1 expression was ensured by sorting the cells by fluorescence activated cell system (FACS) gated on the same level of fluorescence intensity.

The expression levels of OATP2B1 were also examined by fluorescence microscopy. The results confirmed that the recombinant cell lines $HEK_{OATP2B1WT}$ and $HEK_{OATP2B1var}$ both overexpressed OATP2B1 influx protein. Indeed, a bright red fluorescence of the cells overexpressing is observed in $HEK_{OATP2B1WT}$ and variant whereas no fluorescent signal is observed for the control cells (HEK_{CTRL}) (Fig. 1a-f). Furthermore, a strong encircling fluorescent signal is observed indicating a dominant membrane location of the transporters.

Generation of stable $SLCO2B1_{935G/A}$ and $ABCC1_{2012G/T}$ double transfectants cell lines and characterization of protein expression level

As described in the material and methods section, double transfectants were generated by transfecting cells already expressing stably OATP2B1 with pcDNA3.1-eGFP *ABCC1* expression vectors (either WT or variant). As for single transfectants, similar protein expression was ensured by sorting the cells by FACS gated on the same level of fluorescence intensity. This was confirmed through inverted fluorescence

microscopy where all double transfectants express a green and a red fluorescence compared to HEK_{CTRL} cells (Fig. 2a-l). This observation confirms that both influx and efflux proteins are overexpressed in our double transfectant cell models.

Effect of $SLCO2B1_{935G}$ **versus** $SLCO2B1_{935A}$ **overexpression on ATV intracellular accumulation**

Results presented in Fig. 3 compare the ATV intracellular accumulation between $HEK_{OATP2B1WT}$, $HEK_{OATP2B1var}$ and HEK_{CTRL}. After 2h of drug incubation, ATV cellular content is significantly increased in $HEK_{OATP2B1\ WT}$ compared to $HEK293_{CTRL}$ cells from 25nM onwards (*P< 0.05 at 25nM, **P< 0.01 at 50nM, ****P< 0.0001 from 75nM of ATV). Interestingly, $HEK_{OATP2B1var}$ showed a reduced ATV accumulation when compared to its WT counterpart and the difference is significant at 150nM and 500nM. ($^{\#\#}P$< 0.01 at 150nM and $^{\#\#\#}P$< 0.001 at 500nM).

Effect of $SLCO2B1_{935G/A}$ **and** $ABCC1_{2012G/T}$ **co-expression on ATV intracellular accumulation**

After 2h of incubation with increasing concentrations of ATV, the percentage of accumulation in HEK293 control cells is lower compared to every other cell line (Fig. 4a, b). By contrast, intracellular accumulation in single transfectant $HEK_{OATP2B1WT}$ was higher than values observed for all other cell lines whatever the conditions.

Interestingly, MRP1WT activity reduces the increased accumulation generated through OATP2B1WT influx (Fig. 4a). Indeed, the intracellular ATV accumulation in $HEK_{OATPWT-MRP1WT}$ double transfectant is significantly lower than in $HEK_{OATP2B1WT}$ but still significantly higher than in $HEK293_{CTRL}$ cells (*P< 0.05 at 75nM and **** P< 0.0001 from 100nM of ATV) (Fig. 4a).

Moreover, expression of one of the two variant proteins in the models $HEK_{OATP2B1var-MRP1WT}$ or $HEK_{OATP2B1WT-MRP1var}$ significantly reduces the intracellular ATV accumulation compared to the wild-type double transfectant model $HEK_{OATP2B1WT-MRP1WT}$ (**P< 0.01 at 75nM, ***P= 0.001 at 100nM and ****P< 0.0001 from 150nM for $HEK_{OATP2B1var-MRP1WT}$ and $^{\#\#\#\#}P$< 0.0001 from 100nM of ATV for $HEK_{OATP2B1WT-MRP1var}$).

Effect of $ABCC1_{2012G/T}$ **and** $SLCO2B1_{935G/A}$ **co-expression on atorvastatin efflux**

As expected, HEK_{CTRL} showed the weakest efflux ratio, compared to the three tested double transfected cell lines (Fig. 5). From 60 minutes of efflux time onwards, a non-significant trend (P> 0.05) of a higher efflux ratio for the double transfectant model $HEK_{OATP2B1WT-MRP1var}$ was observed compared to cell lines expressing a WT form of the MRP1 ($HEK_{OATP2B1WT-MRP1WT}$ and $HEK_{OATP2B1var-MRP1WT}$). Both cell lines expressing MRP1 WT are characterized by an intermediate efflux ratio. Interestingly, the variant in OATP2B1 does not seem to impact the efflux ratio. This observation is consistent with the fact that OATP2B1 is an influx transporter and is thus expected to impact on accumulation after 120min rather than on drug efflux.

Discussion

Increasing evidence supports the implication of transporters in the biodistribution of drugs. However, little information is available on the local cellular consequences of their expression and on the functional relevance of SNPs for explaining differences in drug intracellular accumulation. In the present study, we have generated different recombinant models overexpressing proteins assumed to play an important role in the local PK of ATV. Indeed, OATP2B1 and MRP1 are both expressed at the skeletal muscle tissue membrane [11] where ATV dose-dependent toxicity is exerted. Going one step further, we have introduced SNPs in the coding sequences of both transporters and created single and double transfectant models allowing to weight the relative importance of their respective activities and evaluating the importance of common genetic polymorphisms.

The principal observations that arise from our investigations are likely to be of importance as we (i) confirm the implication of both OATP2B1 influx and MRP1 efflux transporters in the cellular disposition of ATV, (ii) demonstrate that MRP1 efflux activity counteracts the ATV influx generated by OATP2B1 (iii) show that both investigated SNPs rs12422149 and rs45511401 affect the transporters' activity towards ATV, with rs12422149 being associated with a lower OATP2B1 influx and, rs45511401 with a higher MRP1 efflux, respectively.

Indeed, first, in single transfectant models, we showed that OATP2B1 overexpression increased intracellular ATV accumulation confirming its implication in ATV cellular trafficking. We also observed that the rs12422149 SNP decreases this boosting effect, suggesting a defective effect on its activity. Secondly, our results in double transfectant models demonstrate that MRP1 efflux activity reduces the increased accumulation generated through OATP2B1 influx and even more effectively when the rs45511401 SNP was introduced in *ABCC1* coding sequence. These observations suggest that the efflux activity of MRP1 seems to be boosted by the SNP as, for a comparable OATP2B1 activity (OATP2B1WT), the accumulation is lower in $HEK_{OATP2B1WT-MRP1var}$ when compared to $HEK_{OATP2B1WT-MRP1WT}$. Efflux kinetics experiment corroborates the results of accumulation experiments, and by such, consolidate our assumption of an increased activity of the *ABCC1* variant (rs45511401). On the opposite, the SNP introduced in *SLCO2B1* coding sequence seems to decrease the OATP2B1 influx activity as, for a comparable MRP1 activity (MRP1WT), the accumulation in $HEK_{OATP2B1var-MRP1WT}$ is lower when compared to $HEK_{OATP2B1WT-MRP1WT}$. This observation also confirms results obtained in the single transfectant model with $HEK_{OATP2B1WT}$ and $HEK_{OATP2B1var}$.

The observation that ATV is being transported by the influx protein OATP2B1 is in accordance with the study of Grube *et al*. [23]. Concerning the effect of the rs12422149 *SLCO2B1* SNP, to our knowledge, this is the first study evaluating the effect of this SNP on the activity of the transporter towards ATV either *in vitro* or *in vivo*. When considering other statins, in a mixed cohort of 34 healthy individuals and 40 patients, Tsamandouras *et al*. showed that the rs12422149 SNP in *SLCO2B1* was associated with an increased apparent simvastatin acid clearance using population PK modeling [19]. The authors concluded that this missense polymorphism may be linked to a lower distribution of simvastatin acid in

OATP2B1-expressing tissues explained by a decreased OATP2B1 influx leading to a paradoxical higher elimination rate. Following the same idea, Kim *et al.* highlighted in 2017 that, in 18 volunteers, carriers of the rs12422149 *SLCO2B1* SNP, rosuvastatin was less effective at reducing LDL-cholesterol after 8 weeks of treatment ($P = 0.012$) [20]. This consequence was explained by a reduced OATP2B1 influx transport of the drug into the hepatocytes leading to reduced efficacy of rosuvastatin and increased levels of the drug in the blood circulation. It is important to stress that OATP2B1 has higher expression levels in the liver than in the muscle and is also expressed at lower levels in the lungs and in the placenta. However, to our knowledge, OATP2B1 is the only ATV-influx transporter expressed in the skeletal muscle tissue. Considering this large tissue distribution, the resulting consequences of this SNP, at the systemic level, are difficult to predict. Indeed, on the one hand, a decreased distribution of the drug in peripheral tissues where the protein is expressed (*e.g.* the skeletal muscle and the lungs) is expected. Whereas, on the other hand, the decreased OATP2B1 influx activity in the hepatocytes would reduce the hepatic uptake and by consequence, the active fraction along with the drug clearance [24], leading in all cases to a higher systemic exposure. However, it is important to stress that, in the hepatic tissue, other influx transporters known to be implicated in the hepatic uptake of statins are expressed, such as OATP1B1 or 1B3 and could eventually compensate the decreased OATP2B1 activity. As a consequence, and given the lack of OATP1B1 and OATP1B3 expression in the skeletal muscle tissue, one can speculate that the functional defect caused by this SNP would have more impact on local exposure (*i.e.* in the myocytes) where no other influx transporters can compensate the consequent decreased influx activity than on the systemic clearance where other transporter can compensate for this decreased activity [25].

We also highlighted that the rs45511401 SNP (c.2012G > T) in *ABCC1* was associated with an apparent gain of efflux activity of MRP1 towards ATV using our double transfectant models, suggesting that this SNP would protect against ATV intracellular accumulation. By contrast, in single transfectant MRP1 model, no effect of MRP1 efflux was shown on ATV accumulation (data not shown). This might be due to the fact that the affinity (Km) of the transporter is too low and requires a prior activity of an influx of drug to assess its implication in the drug transportation. This observation agrees with the *in vitro* study of Knauer *et al*. which showed that the impact of MRP1 activity is significant only when co-expressed with a rodent-Oatp2b1 [11]. Few data are available about the impact of this *ABCC1* SNP on ATV transport. Nevertheless, in 2017, Behdad *et al.* reported a study of 179 patients with primary hypercholesterolemia relating the impact of rs45511401 in *ABCC1* and rs1045642 in *ABCB1* on the clinical response to ATV. The investigation did not reveal any significant difference in lipid-lowering response when comparing patients expressing the *ABCC1* wild-type or variant genotype [26]. As for OATP2B1, the lack of significant effect on systemic exposure and on the LDL-cholesterol lowering effect does not exclude a local PK effect as the protein is more importantly expressed in peripheral tissues, especially in the skeletal muscle tissue. Indeed, transcriptomics data revealed *ABCC1* relative mRNA expression level of 1.552 transcripts per million (TPM) in the liver whereas levels are 10-fold higher in the skeletal muscle (15.65 TPM), arguing in the sense of a pronounced local rather than a systemic effect (GTEx Portal) [27]. To our knowledge, no study evaluated the impact of both SNPs, either in *ABCC1* or in *SLCO2B1*, on the susceptibility to present ATV-related muscle side effects.

All in all, our results consistently demonstrates that the intracellular PK of ATV is ruled by the local expression and activity of drug transporters and that OATP2B1 and MRP1 are likely to play a significant role in this bidirectional dynamic. We showed that MRP1 efflux activity toward ATV protects against its high accumulation generated through OATP2B1- influx. This observation might be linked to a protection towards ATV-related toxicity at the skeletal muscle tissue level. We have also shown that SNPs present in the coding sequences of these transporters might impact on their activity and modulate the intracellular accumulation of their substrates that might be associated with the susceptibility to suffer from muscle discomfort. These results constitute a first step in the understanding of inter-individual variabilities in ATV PK that could explain muscular side effects individual susceptibilities.

Methods

Materials

Atorvastatin (ATV) was purchased from Pfizer (New York, NY) and the d5-ATV calcium salt from Alsachim (CAS number: 222412-82-0). Gentamicin (G418), hygromycin B, dimethyl sulfoxide (DMSO), ampicillin and kanamycin were purchased from Sigma-Aldrich (St. Louis, MO).

Cell culture

Human Embryonic Kidney cells (HEK 293, ATCC N°CRL-1573) control and transfected cells were grown in Dulbecco's Modified Eagle Medium with high glucose, L-glutamine and sodium pyruvate (DMEM GIBCO®) supplemented with 10% (v/v) Fetal Bovine Serum (FBS) and 1% (v/v) of penicillin-streptomycin purchased from ThermoFisher Scientific (Waltham, MA). Cells were cultured at 37°C with 5% CO_2. For re-culturing, cells were detached with enzyme-free cell dissociation buffer (ThermoFisher Scientific).

Generation of *SLCO2B1*$_{935G}$ and *SLCO2B1*$_{935A}$ plasmids

The expression vector pCMV-V-OFPSpark® coding for the wild-type OATP2B1 protein (SLCO2B1$_{935G}$) and a fluorescent red tag (OFPSpark®) was purchased from Bio-Connect life sciences (cat. HG18756-ACR, Huissen, The Netherlands). The construct is resistant to bacterial (kanamycin) and eukaryotic (hygromycin B) antibiotics, allowing further bacterial and cell selection. The variant plasmid expressing SLCO2B1$_{935A}$ (rs12422149), was generated by site-directed mutagenesis directed by PCR (Icycler IQ - BioRad, Hercules, CA) using Phusion Site-Directed Mutagenesis kit (Waltham, MA) following the manufacturer's protocol. The back-to-tail primers phosphorylated in 5'-OH that include the point mutation were 5'-CAG TTT CGG CAA AAG GTC TTA G-3' (forward) and 5'-AAG CTC ACG TTT TTC CTT G-3' (reverse) and were purchased from Eurofins Scientific SE (Ebersberg, Germany). The plasmid transformation and amplification were performed in dH5$_\alpha$ Escherichia Coli strains through Heat-Shock. The product was then purified by maxiprep using the PureLink™ HiPure Plamid Filter Maxiprep (ThermoFisher Scientific, Waltham, MA). The amplicon was finally sequenced using Sanger method (Eurofins, Germany) to confirm

the introduction of the point mutation c.935G>A in the coding nucleotide sequence of *SLCO2B1* (Fig. 6a, b).

Generation of $ABCC1_{2012G}$ and $ABCC1_{2012T}$ plasmids

The expression vector pcDNA3.1-eGFP was kindly offered by Dr. Susan Cole (PMID: 24080162), and codes for the wild-type MRP1 protein ($ABCC1_{2012G}$) with a green fluorescent tag (GFP). The construct is resistant to bacterial (ampicillin) and eukaryotic (gentamicin) antibiotics, allowing further bacterial and cell selection. As for *SLCO2B1*, the variant plasmid expressing $ABCC1_{2012T}$ (rs45511401) was generated by site-directed mutagenesis directed by PCR. The back-to-tail primers phosphorylated in 5'-OH that include the point mutation were 5'-ATC CCC GAA GTT GCT TTG GTG-3' (forward) and 5'-GGA GAA GGT GAT GCC ATT C-3' (reverse). The product was amplified and purified in the same conditions as previously described and the variant was successfully introduced in the coding sequence of *ABCC1*. (Fig. 6c, d)

Generation of stable recombinant cell lines

For single transfectants overexpressing either the wild-type (WT) or the variant (var) OATP2B1 protein, *i.e.* $HEK_{OATP2B1WT}$ and $HEK_{OATP2B1var}$, 5 x 10^5 HEK293 cells/well were seeded in 12-well plates the day before the transfection with lipofectamine 3000 Transfection Kit (Invitrogen, Carlsbad, CA) with 1.25µg of plasmid DNA (either $SLCO2B1_{935G}$ or $SLCO2B1_{935A}$ plasmids*)*. The same method was used to obtain HEK_{MRP1WT} and $HEK_{MRP1var}$ single transfectants. For the double transfectants, 1 x 10^6 cells already overexpressing one of the two proteins (either $HEK_{OATP2B1WT}$ or $HEK_{OATP2B1var}$) were cultured in 6-well plates one day before the lipofection. Transfection was then achieved using 2.5µg of plasmid DNA per well (either $ABCC1_{2012G}$ or $ABCC1_{2012T}$ plasmids). The antibiotic selection was performed 72h post-lipofection with hygromycin B and G418 at a final concentration of 0.5 mg/ml and 1mg/ml to select cells that stably expressed OATP2B1 and/or MRP1 proteins, respectively. Resistant strains were reseeded after 14 days for future development and sorted by flow cytometry.

Double transfectant models will be renamed thereafter with the model overexpressing both WT transporters being $HEK_{OATP2B1WT\text{-}MRP1WT}$, the model overexpressing *SLCO2B1* WT and *ABCC1* variant; $HEK_{OATP2B1WT\text{-}MRP1var}$, and the model overexpressing *SLCO2B1* variant and *ABCC1* WT; $HEK_{OATP2B1var\text{-}MRP1WT}$. According to the relatively low frequency of the polymorphisms in the population, the impact of both mutations in the double transfectant model $HEK_{OATP2B1var\text{-}MRP1var}$ was not investigated (theorical frequency of the combination is 0.66%).

Characterization of OATP2B1 and MRP1 protein expression

Flow cytometry

Cells were detached, counted and centrifuged at 400g for 5 minutes at 4°C on the day of the experiment. The supernatant was discarded and the cell pellet resuspended in 2mL of sterile FACS-Buffer (Dulbecco's PBS, 1% (v/v) decomplemented FBS, 1mM EDTA [ThermoFischer Scientific]). Cells were washed twice then resuspended either in FACS-buffer for analysis with BD-FACS Verse or sorting with BD FACSAria® III (BD Biosciences, New Jersey). OFPSpark® (red OATP2B1) and eGFP (green MRP1) fluorescence were excited with the blue laser (488nm) with bandpass filters that were BP 586/42 and 527/32 respectively. Raw data were analyzed using the FlowJo software (Ashland, OR). Since fluorescent OFPSpark® and eGFP emission spectra partially overlap, data were compensated through FlowJo.

All generated recombinant models were sorted with fluorescence parameters gated on the same level of intensity to ensure similar protein expression. Sorted cells were reseeded in 12-well plates with the adequate selective antibiotic concentrations to allow growth expansion.

Inverted fluorescence microscope

Cells were seeded in Ibidi 4 chambers pH+ µ-slide (Gräfelfing, Germany) 48h prior to microscopy analysis using Zeiss Observer Z1 (Zeiss, Germany). Fluorescent signal was obtained using Zeiss Colibri 7 LED light source. The red fluorescence (OFPSpark®) emitted by the tag attached to OATP2B1 was observed with the yellow LED at an excitation of 555nm and an emission QBP 582/30. The green fluorescence (eGFP) emitted by the tag attached to MRP1 was observed with the blue LED at an excitation of 475nm and an emission QBP 514/30. Images were taken with Zeiss Axiocam 506 mono and processed with Zeiss Zen 2 lite software.

Characterization of OATP2B1 and MRP1 activity

Atorvastatin intracellular accumulation and efflux kinetics

The day before the accumulation, cells (3×10^5) were seeded in 24-well plates coated with poly-L-lysine (Sigma-Aldrich), reaching a confluence of ~90% the next day. The day of the experiment, 50µL of each well were removed before the addition of 50µL of freshly diluted ATV solution. For drug accumulation, cells were incubated for 120 minutes with increasing ATV concentrations (0, 50, 75, 100, 150 and 500nM) whereas a concentration of 75nM was selected for the efflux kinetics. All experiments were performed at least twice (N=2) and in triplicate (n=3). After ATV incubation at 37°C with 5% of CO_2 saturation, plates were centrifuged (Eppendorf 417R) at 400g for 5 minutes at 4°C and the supernatant was discarded. Cells were washed three times with 500µL of ice-cold D-PBS and either recovered for accumulation experiments or allowed to efflux in a drug-free medium for 30, 60, 120, 300 minutes. Cells were finally resuspended in 500µL of D-PBS supplemented with 1mM EDTA, transferred to a 1.5ml Eppendorf® (Hamburg, Germany) and centrifuged at 400g for 5 minutes at 4°C. The supernatant was finally discarded and the cell pellet stored at -20°C for further extraction. For efflux kinetics, aliquots of media (500µl) were collected at each time point to quantify the fraction of drug effluxed as well as the cell pellet collected with the same method previously described. The efflux ratio was calculated by normalizing the

amount of effluxed ATV in the medium at the time points (30, 60, 120 or 300 min) on the intracellular amount accumulated at the start of the efflux period (i.e. after 2h of accumulation).

Atorvastatin extraction and quantification

Thawed cell pellets were resuspended in 100µL of extraction solvent constituted of a mix of methanol-water (60:40, v/v) and d5-ATV at a final concentration of 5nM. Samples were vortexed then sonicated for 10 minutes and centrifuged during 5 minutes at 10,600g at room temperature. The cell pellets were stored at -20°C for protein assay and supernatants were transferred to an injection vial and dried under nitrogen flow. The residue was resuspended in 30µL of methanol before injection in the HPLC-MS/MS system. For ATV media quantification, 500µl of media were added to 1.2mL of ice-cold acetone supplemented with d5-ATV at a final concentration of 5nM. The mix was vigorously vortexed and stored at -20°C for 2h and then centrifuged at 10,600g for 10 minutes. The supernatant was subsequently evaporated and resuspended in MeOH. 5µL of each extract was injected in the HPLC-MS/MS system (Xevo TQ-S, Waters). Analyte separation was obtained using a gradient between mobile phase A (MeOH-H_2O (75:25) with 0.1% (v/v) of acetic acid) and mobile phase B (MeOH with 0.1% (v/v) of acetic acid) and a UPLC column (Ascentis Express C18 column (2.7µm, 150x4mm)) equipped with a pre-column. For MS/MS detection, ionized compounds were generated using an electrospray source operated in positive mode. Detection was performed by Multiple Reaction Monitorinig (MRM) mode using the quantification transitions 564.3 à 440.3 for d5-ATV and 559.2 à 440.2 for ATV. Calibration curves were established between 0.5 and 1000 fmol of ATV on column. Data analysis was performed on MassLynx software (Waters). ATV concentrations were normalized on the total protein content.

Protein normalization and statistical analysis

Protein assay was performed in triplicate for each sample with thawed cell pellet using DC™ Protein Assay (BioRad, Hercules, CA).

Graphs and statistical analysis were realized with GraphPad Prism 8.4.2. To assess transporters impact on ATV intracellular accumulation, ANOVA-2 ways was used to evaluate the impact of 2 independent factors, *i.e.* ATV incubation concentrations (accumulation experiment) or efflux time (efflux kinetics) and the cell lines. Bonferroni post-hoc tests were performed for multiple comparisons in order to determine which mean differed from the others. In all cases, results were considered significant when p-value was < 0.05.

Declarations

Acknowledgements

The authors wish to thank Mr. Dauguet Nicolas and Pr. Van der Smissen (CYTF and CELL/DDUV UCLouvain) for their outstanding help at the FACS and the fluorescence microscopy platforms, respectively.

This work was supported by Fonds pour la Formation à la Recherche dans l'Industrie et dans l'Agriculture (FRIA) under the Grant Number FC33437 to Hoste E., and by grants from the Fonds national de la Recherche scientifique [FRS-FNRS] (Grants J018317 and J006920).

Author contributions

E.H., V.H. and L.E. designed the research; E.H., N.P. and H.E.H. conducted the experiments; E.H., N.P. and S.H. designed the cell models; A.P. and G.G.M. performed the HPLC/MS-MS analysis; E.H., V.H. and L.E. drafted the manuscript and all authors reviewed and approved the final version of the document.

Availability of data and materials

Observations related to rs12422149 and rs45511401 SNPs have been deposited in ClinVAR awaiting accession numbers (refs: SUB11349669 and SUB11332554).

Data availability statement

All experimental data generated and/or analyzed during the study are available from the corresponding author on reasonable request.

Competing interests

The authors declare no conflicts of interest.

References

1. Adams, S. P., Tsang, M. & Wright, J. M. Lipid lowering efficacy of atorvastatin. *Cochrane Database Syst. Rev.* **12**, Cd008226, doi:10.1002/14651858.CD008226.pub2 (2012).
2. Jacobson, T. A., Schein, J. R., Williamson, A. & Ballantyne, C. M. Maximizing the cost-effectiveness of lipid-lowering therapy. *Arch. Intern. Med.* **158**, 1977-1989, doi:10.1001/archinte.158.18.1977 (1998).
3. Bruckert, E., Hayem, G., Dejager, S., Yau, C. & Bégaud, B. Mild to moderate muscular symptoms with high-dosage statin therapy in hyperlipidemic patients--the PRIMO study. *Cardiovasc. Drugs Ther.* **19**, 403-414, doi:10.1007/s10557-005-5686-z (2005).
4. Cohen, J. D., Brinton, E. A., Ito, M. K. & Jacobson, T. A. Understanding Statin Use in America and Gaps in Patient Education (USAGE): an internet-based survey of 10,138 current and former statin users. *J. Clin. Lipidol.* **6**, 208-215, doi:10.1016/j.jacl.2012.03.003 (2012).
5. Baker, S. K. Molecular clues into the pathogenesis of statin-mediated muscle toxicity. *Muscle & nerve* **31**, 572-580, doi:10.1002/mus.20291 (2005).
6. Sakamoto, K., Honda, T., Yokoya, S., Waguri, S. & Kimura, J. Rab-small GTPases are involved in fluvastatin and pravastatin-induced vacuolation in rat skeletal myofibers. *Faseb j.* **21**, 4087-4094, doi:10.1096/fj.07-8713com (2007).

7. Morikawa, S.*et al.* Analysis of the global RNA expression profiles of skeletal muscle cells treated with statins. *Journal of atherosclerosis and thrombosis* **12**, 121-131, doi:10.5551/jat.12.121 (2005).
8. Norata, G. D., Tibolla, G. & Catapano, A. L. Statins and skeletal muscles toxicity: from clinical trials to everyday practice. *Pharmacological research* **88**, 107-113, doi:10.1016/j.phrs.2014.04.012 (2014).
9. Ownby, S. E. & Hohl, R. J. Farnesol and geranylgeraniol: prevention and reversion of lovastatin-induced effects in NIH3T3 cells. *Lipids* **37**, 185-192, doi:10.1007/s11745-002-0879-1 (2002).
10. Lennernas, H. Clinical pharmacokinetics of atorvastatin. *Clinical pharmacokinetics* **42**, 1141-1160, doi:10.2165/00003088-200342130-00005 (2003).
11. Knauer, M. J.*et al.* Human skeletal muscle drug transporters determine local exposure and toxicity of statins. *Circulation research* **106**, 297-306, doi:10.1161/circresaha.109.203596 (2010).
12. Rosenberg, M. F.*et al.* The structure of the multidrug resistance protein 1 (MRP1/ABCC1). crystallization and single-particle analysis. *J. Biol. Chem.* **276**, 16076-16082, doi:10.1074/jbc.M100176200 (2001).
13. Choudhuri, S. & Klaassen, C. D. Structure, function, expression, genomic organization, and single nucleotide polymorphisms of human ABCB1 (MDR1), ABCC (MRP), and ABCG2 (BCRP) efflux transporters. *Int. J. Toxicol.* **25**, 231-259, doi:10.1080/10915810600746023 (2006).
14. Conseil, G. & Cole, S. P. Two polymorphic variants of ABCC1 selectively alter drug resistance and inhibitor sensitivity of the multidrug and organic anion transporter multidrug resistance protein 1.*Drug Metab. Dispos.* **41**, 2187-2196, doi:10.1124/dmd.113.054213 (2013).
15. Nies, A. T.*et al.* Genetics is a major determinant of expression of the human hepatic uptake transporter OATP1B1, but not of OATP1B3 and OATP2B1. *Genome Med.* **5**, 1, doi:10.1186/gm405 (2013).
16. König, J., Cui, Y., Nies, A. T. & Keppler, D. A novel human organic anion transporting polypeptide localized to the basolateral hepatocyte membrane. *Am. J. Physiol. Gastrointest. Liver Physiol.* **278**, G156-164, doi:10.1152/ajpgi.2000.278.1.G156 (2000).
17. Kullak-Ublick, G. A.*et al.* Organic anion-transporting polypeptide B (OATP-B) and its functional comparison with three other OATPs of human liver. *Gastroenterology* **120**, 525-533, doi:10.1053/gast.2001.21176 (2001).
18. Kinzi, J., Grube, M. & Meyer Zu Schwabedissen, H. E. OATP2B1 - The underrated member of the organic anion transporting polypeptide family of drug transporters? *Biochem. Pharmacol.* **188**, 114534, doi:10.1016/j.bcp.2021.114534 (2021).
19. Tsamandouras, N.*et al.* Identification of the effect of multiple polymorphisms on the pharmacokinetics of simvastatin and simvastatin acid using a population-modeling approach. *Clin. Pharmacol. Ther.* **96**, 90-100, doi:10.1038/clpt.2014.55 (2014).
20. Kim, T. E.*et al.* The Effect of Genetic Polymorphisms in SLCO2B1 on the Lipid-Lowering Efficacy of Rosuvastatin in Healthy Adults with Elevated Low-Density Lipoprotein.*Basic Clin. Pharmacol. Toxicol.* **121**, 195-201, doi:10.1111/bcpt.12826 (2017).

21. Ensembl.org. *rs12422149*, <https://www.ensembl.org/Homo_sapiens/Variation/Population?db=core;r=11:75172032-75173032;v=rs12422149;vdb=variation;vf=168665315> (2021).
22. Ensembl.org. *rs45511401*, <https://www.ensembl.org/Homo_sapiens/Variation/Population?db=core;v=rs45511401;vdb=variation> (2021).
23. Grube, M.*et al.* Organic anion transporting polypeptide 2B1 is a high-affinity transporter for atorvastatin and is expressed in the human heart.*Clin. Pharmacol. Ther.* **80**, 607-620, doi:10.1016/j.clpt.2006.09.010 (2006).
24. Stillemans, G.*et al.* Atorvastatin population pharmacokinetics in a real-life setting: Influence of genetic polymorphisms and association with clinical response.*Clin Transl Sci* **15**, 667-679, doi:10.1111/cts.13185 (2022).
25. MA, V. W.*et al.* Genetic variation in statin intolerance and a possible protective role for UGT1A1. *Pharmacogenomics* **19**, 83-94, doi:10.2217/pgs-2017-0146 (2018).
26. Behdad, N., Kojuri, J., Azarpira, N., Masoomi, A. & Namazi, S. Association of ABCB1 (C3435T) and ABCC1 (G2012T) Polymorphisms with Clinical Response to Atorvastatin in Iranian Patients with Primary Hyperlipidemia. *Iran Biomed. J.* **21**, 120-125, doi:10.18869/acadpub.ibj.21.2.120 (2017).
27. GTExPortal.org. *Bulk tissue gene expression for ABCC1*, <https://www.gtexportal.org/home/gene/ABCC1> (2021).

Figures

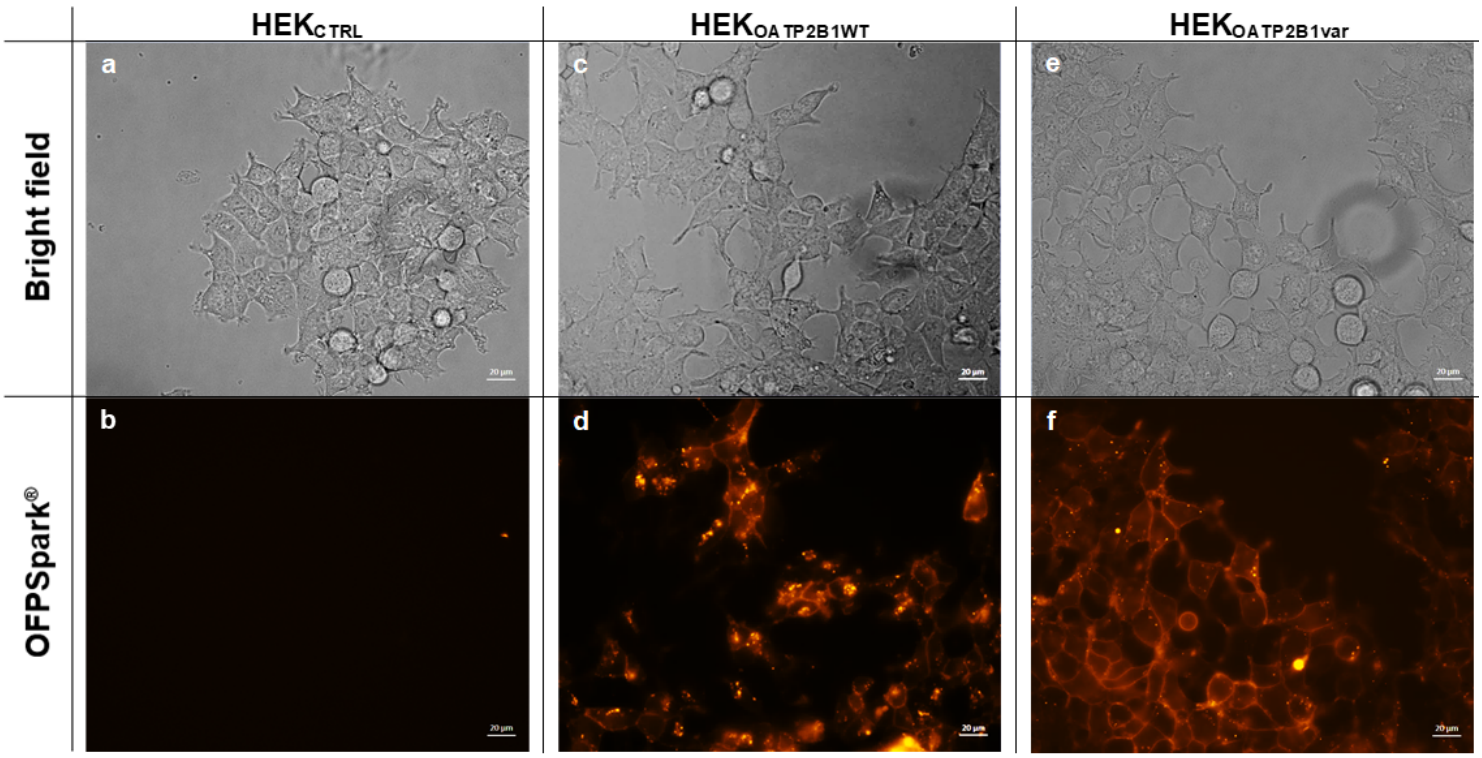

Figure 1

Fluorescence microscopy (**a, b**) HEK_{CTRL}, (**c, d**) recombinant $HEK_{OATP2B1WT}$ and (**e, f**) recombinant $HEK_{OATP2B1var}$ in bright field above and in red OFPSpark® detection below.

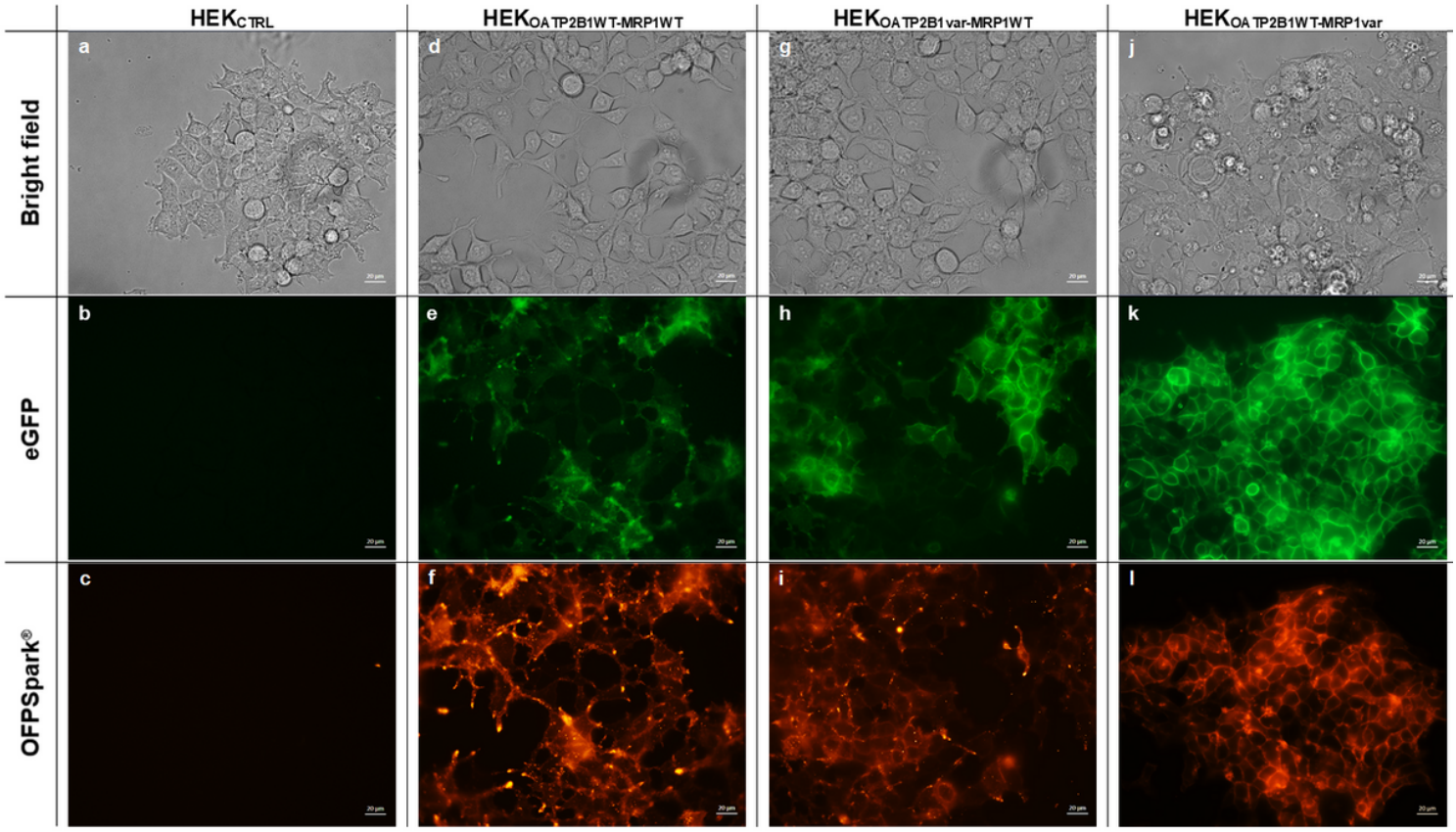

Figure 2

Fluorescence microscopy (**a-c**) HEK_{CTRL}, (**d-f**) recombinant $HEK_{OATP2B1WT-MRP1WT}$, (**g-i**) recombinant $HEK_{OATP2B1var-MRP1WT}$ and (**j-l**) recombinant $HEK_{OATP2B1WT-MRP1var}$ in bright field above, in green eGFP detection centered and in red OFPSpark® detection below.

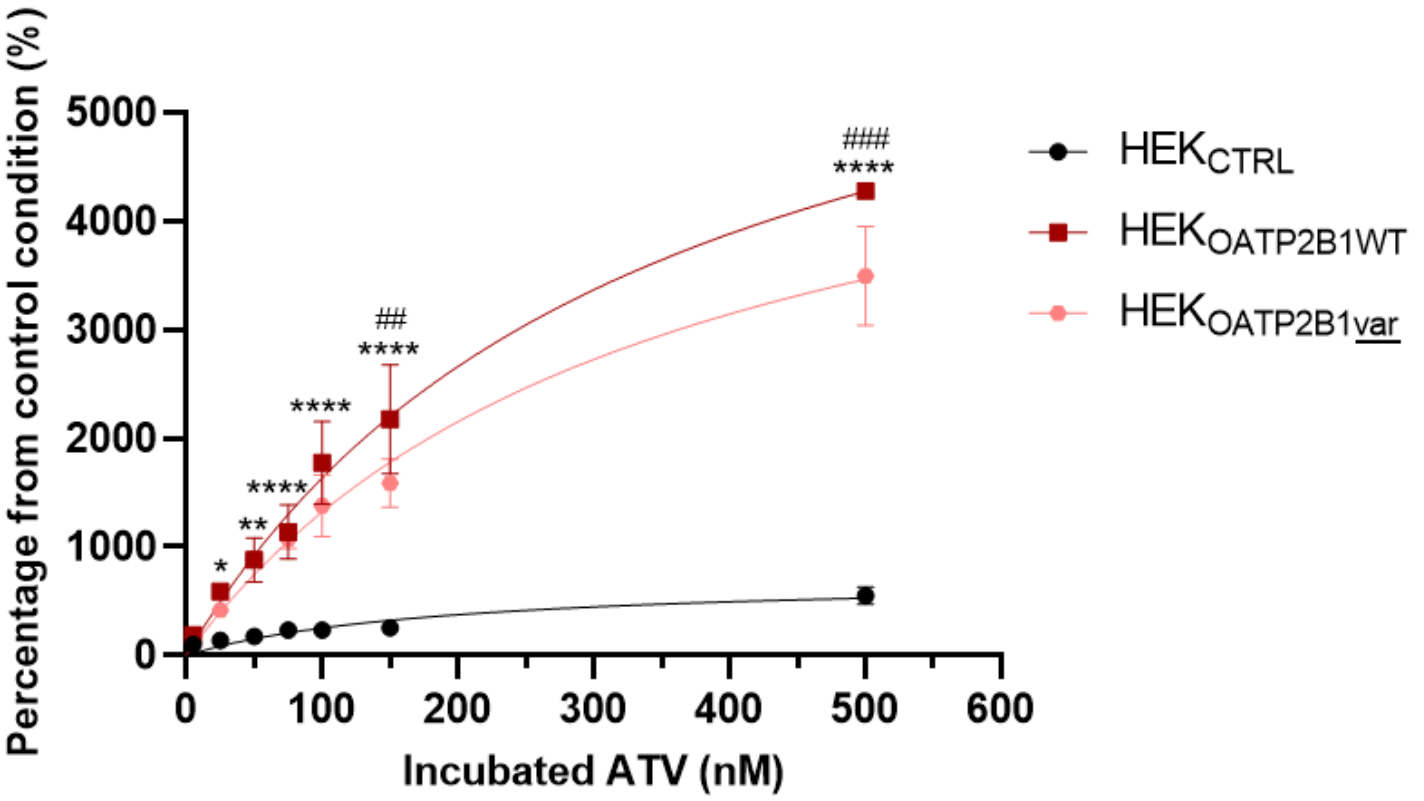

Figure 3

ATV accumulation experiment represented in percentage from the control condition (ATV accumulation in HEK_{CTRL} at the lowest concentration) in single transfectant models $HEK_{OATP2B1WT}$ and $HEK_{OATP2B1var}$ compared to the control cells HEK_{CTRL}. (*$P < 0.05$, **$P < 0.01$, ****$P < 0.0001$ $HEK_{OATP2B1WT}$ compared to HEK_{CTRL} and $^{\#\#}P < 0.01$, $^{\#\#\#}P < 0.001$ $HEK_{OATP2B1var}$ compared to HEK_{CTRL}).

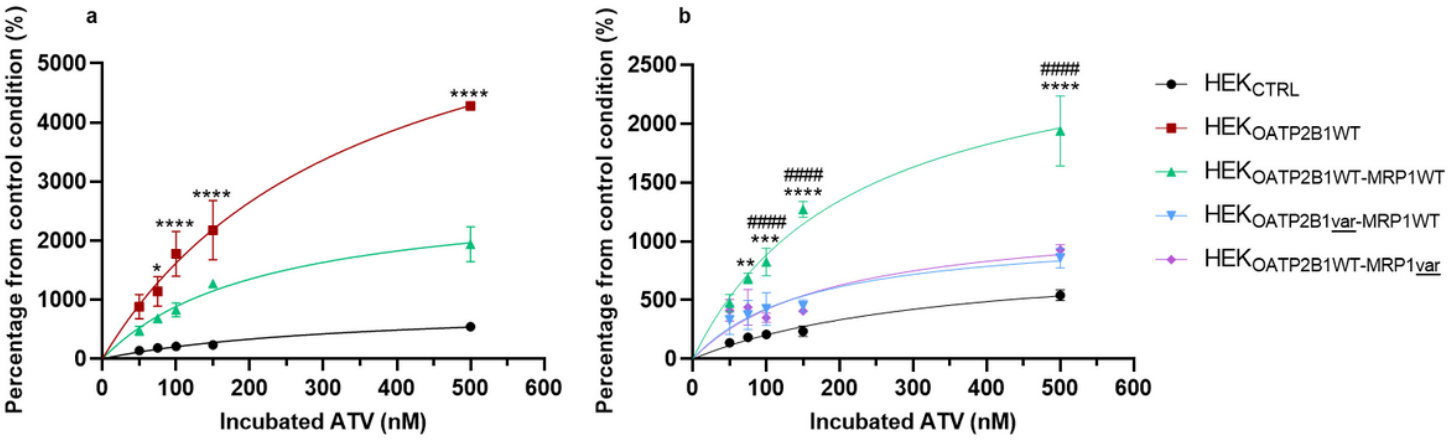

Figure 4

ATV accumulation experiment represented in percentage of accumulation from the control condition (ATV accumulation in HEK_{CTRL} at the lowest concentration) in (**a**) single transfectant $HEK_{OATP2B1WT}$ vs. double transfectant $HEK_{OATP2B1WT\text{-}MRP1WT}$ and vs. HEK_{CTRL} (*P < 0.05, **** P < 0.0001 compared to double transfectant WT model) and in (**b**) double WT transfectant vs. variant models. (**P < 0.01, ***P < 0.001, **** P < 0.001 compared to $HEK_{OATP2B1var\text{-}MRP1WT}$ model and $^{\#\#\#\#\#}P$ < 0.0001 compared to $HEK_{OATPWT\text{-}MRP1var}$).

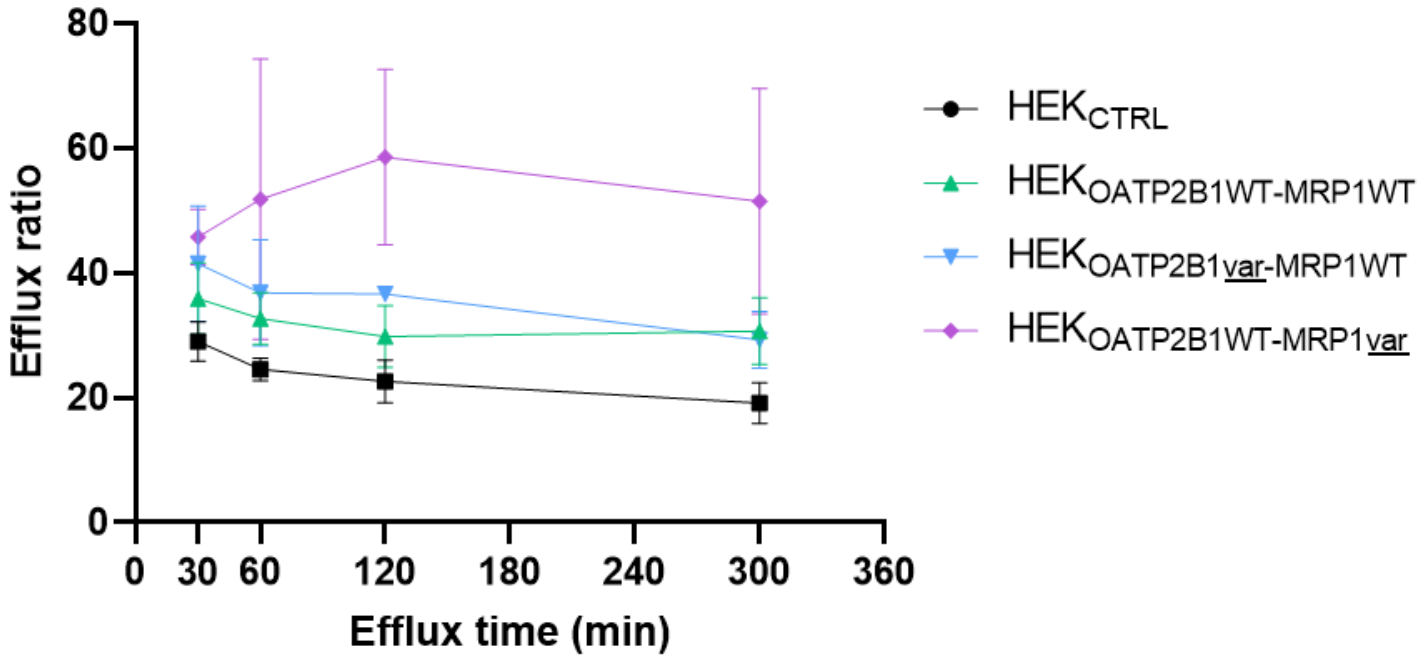

Figure 5

ATV efflux ratio in cell models from 30 to 300 minutes of efflux time. The efflux ratio is reporting the effluxed ATV amount in the media compared to the initial intracellular ATV amount, normalized on protein content. Non-significant results, P > 0.05 with Bonferroni post-hoc tests.

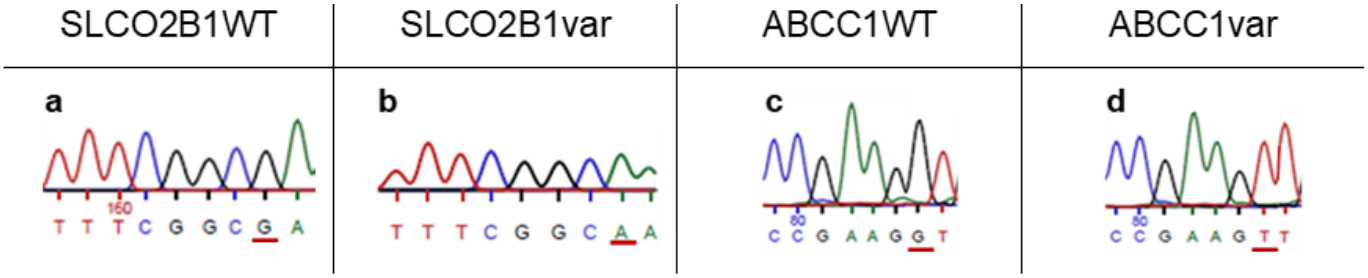

Figure 6

Gene sequencing of HEK293 transfected cells with (**a**) OATP2B1WT, (**b**) OATP2B1var, (**c**) MRP1WT and (**d**) MRP1var.